

## CONCEPTUAL AND AERODYNAMIC DESIGN OF A UAV FOR SUPERFICIAL VOLCANO MONITORING

**P. D. Bravo-Mosquera\*, A. Martins-Abdalla\*, H. D. Ceron-Muñoz\*, F. M. Catalano\*.**  
**\*Aerodynamic Laboratory, São Carlos Engineering School-University of São Paulo-Brazil.**

**Keywords:** *Unmanned Aerial Vehicle, Volcano Monitoring, Conceptual Design, Aerodynamic Design, Computational Fluid Dynamics.*

### Abstract

*Unmanned systems have ideal characteristics to recognize areas of difficult access, performing missions that could not be made with traditional manned aircraft. Hence, nowadays, Unmanned Aerial Vehicles (UAVs) technology has improved considerably.*

*One of the main drawbacks in the monitoring of an active volcano is the inability to fly between a large gas plumes due to the possible entrance of volcanic ash into the aircraft engine.*

*Accordingly, the physical risk of pilots and scientist that investigate volcanoes aboard of an aircraft is great, if an unexpected event occurs.*

*Under these limitations, a UAV design is proposed for superficial volcano monitoring, with the mission to transmit real time data to a remote location, preventing the exposition of people to these flight conditions.*

*The conceptual design process was carried out with the implementation of a parametric study, using statistical entropy and constraint analysis, in order to determine the minimum value of wing area and thrust required to perform the mission. For the aerodynamic design, analytical studies were developed, through the determination of the aerodynamics, performance and longitudinal stability characteristics.*

*Finally, the aerodynamic coefficients of the wing and the full configuration were evaluated with Computational Fluid Dynamics (CFD) simulations. The numerical results are greatly similar in the lift ( $C_L$ ), drag ( $C_D$ ) and moment ( $C_M$ ) coefficients, when these are compared with the analytical results. Consequently, the results show, on a large scale, as would be the aerodynamic behavior of the UAV performing the established mission.*

### 1 Introduction

The study of volcanoes has been of vital importance to society, because these have caused many disasters over time, generating an imminent danger to the nearby towns [1,2]. In this respect, active volcanoes are become in true natural laboratories for the scientists that seek new ways to prevent and handle emergencies.

Gas emission and geographical deformations in volcanoes are warnings of a possible eruption; specialized research centers in the control and prevention of volcanic eruptions have different procedures to analyze the behavior inside and outside the craters, one of these is performed by the continuous flights over the volcanic domes, with the intervention of manned aircraft. Therefore, in these kinds of monitoring, the aircraft are equipped with instruments used to analyze the geographical and thermal changes over the volcano surface.

Nevertheless, these flight conditions are not the most recommended to operate, because the gases and the ash that are emanating constantly, can affect the aircraft performance, risking the lives of the crew aboard [3,4,5,6].

As a solution, in this paper is reported the aerodynamic design of a low-cost UAV called **URCUNINA-UAV** (that means Fire Mountain) to perform flights around volcanoes, with the mission to take pictures and videos at real time from different positions until a safe zone, as well as, gather the CO<sub>2</sub> and SO<sub>2</sub> concentration, to study the toxicity and the temperature of the volcanic gases, aiding to the research centers of volcanoes in its investigations. In relation to this, to start with the conceptual and

aerodynamic design of the **URCUNINA**, it was carried out a rigorous analysis of the field operation, in order to begin with the first design estimations, in relation to some performance characteristics [7].

Therefore, the geographical features of the Galeras Volcano, located in Pasto-Colombia were selected [8,9]. Therefore, the **URCUNINA** must be able to fly up to  $4500m$  above sea level. Under these conditions, an aerodynamic, performance and longitudinal stability analysis for the wing and the full configuration of the **URCUNINA** were developed.

According to the parameters mentioned above, the changes in the Lift and Drag coefficients in the airfoils are very sensitive to the Reynolds Number ( $Re$ ). Hence, different airfoils were studied to determine the best aerodynamic features to perform an adequate mission, where low velocities are required in order to allow taking pictures, videos and gas information at real time over the volcano [10]. Thus, sufficiently high lift coefficient ( $C_L$ )<sub>max</sub> is required. The best airfoil was chosen based on an iterative design process with the wing surface, applying the Prandtl's Lifting Line theory, where some parameters of the airfoil as the lift curve slope, the attack angle at zero lift coefficient and the minimum drag coefficient were required [11,12,13]. The airfoil that achieves the best features was the Eppler 423, it is characterized by two aerodynamic parameters: high lift coefficients at low Reynolds numbers and at high attack angles, without boundary layer detachment [14,15,16].

On the other hand, for the selection of the propulsion system, it took into account the decrease of the mass flow rate at the operation altitude. Therefore, the selected engine/propeller reaches the performance requirements obtained in the conceptual design phase, having the sufficient Thrust to Weight Ratio ( $T/W$ ) to perform the mission.

Finally, the CFD simulations were conducted and the main aerodynamic characteristics were analyzed to foreknow the **URCUNINA** performance in this sort of specific mission.

In the Fig. 1 is showed an artistic image of the **URCUNINA** flying over the Galeras Volcano.



Fig 1. URCUNINA-UAV Artistic image.

## 2 Research Relevance

When the scientists in charge of superficial volcano monitoring do not have the possibility to use aircraft for their studies, normally, it is done by NASA satellites that take pictures at real time, if an eruption or a change in the volcanoes craters is happening. However, it is not possible to know more details and may even generate false alarms. [5,10,17,18] For this reason, new devices capable of measuring volcanic gases are being developed, with the aim to study in situ the volcanoes behavior, using unmanned and manned aircraft vehicles [3,19]. In regard to the above, Diaz and Pieri [3,5,10], Patterson [4] and Caltabiano [19] have been conducting studies of the behavior of volcanoes around the world, implementing their devices in UAVs designed for any other type of mission, among which are: the Wing 100, the Sierra and the Silver Fox. As a result, some aerodynamic problems in mission were presented, e.g. The Wing 100 had an excellent aerodynamic efficiency, due to is a flying wing. However, it suffered the inherent disadvantage of being unstable and difficult to control in flight. In addition, the low payload and endurance capabilities made it unable to perform this type of mission. Moreover, the Sierra and the Silver Fox had an excellent performance in flight. Nevertheless, the wing circulation inside the crater produced a significant turbulence, resulting in the movement backwards of the aircraft, with respect to the ground. This is because the wings of these UAVs were not designed to perform this mission.

On the other hand, Johnson [18] and Weber [20] used manned aircraft in their studies, among which are: the Cessna 206 and the Flight Design

CT, equipped with a piston engine with an air filter, avoiding the entrance of volcanic ash into the engine. The principal advantage of these aircraft was the range and the endurance. However, the dangerous and often remote nature of volcanic plumes could pose a non-trivial risk to the aircrews.

As can be understood, it does not exist in the market an aircraft that have been designed for this specific mission. Therefore, in this paper is presented the conceptual and the preliminary aerodynamic design of a UAV for superficial volcano monitoring, taking into account all the parameters, conditions and constraints mentioned above.

### 3 Conceptual Design

#### 3.1 Statistical Entropy Application

The application of the statistical entropy in this project was to study the evolution of the design variables of UAVs of the same category, which could serve as initial parameter for the conceptual design of the **URCUNINA**.

As stated above, it does not exist in the market an aircraft designed for this type of mission. However, a large research in photographic and environmental UAVs was carried out, making a database with 20 UAVs, in order to analyze the principal design characteristics of each one of these. The analysis of this section is supported by the computational module developed by Abdalla [21]. This tool integrates the concepts of Statistical entropy, Quality function deployment and Genetic algorithm in the application of multidisciplinary optimization as a conceptual design methodology, allowing to know the changes between subsequent designs, with the insertion of a new design in the market. This methodology proves to be objective and balanced when is compared with existing traditional techniques of aircraft conceptual design. Accordingly, each UAV was classified in terms of its characteristics, in four types of designs: Dominant designs, innovative designs, failed designs and monopolized designs. Further information of this stage, is reported in [6].

In regard, the dominant design of the database was the UAV whose geometrical, aerodynamic

and performance features were the basis for the development of the others, this means that, the design parameters of this dominant UAV were highly efficient and reduce the risk factor in the design of new projects of the same category. Considering the results shown in the Fig. 2, the **URCUNINA** was designed taking into account some similar characteristics of the dominant UAV, as well as some geometric and performance characteristics of the innovative UAV. Against this background, the main features for the conceptual design are presented below:

- A Combustion power plant for the propeller was selected, due to it has higher performance in the endurance and range capabilities, this includes a filter to prevent ingress of ash.
- The pusher configuration and front payload nose make it ideal for atmospheric measurements.
- The payload for the mission does not exceed a total weight of 4 Kg.
- The V inverted tail is the design feature more used in the UAVs database, this is due to its stability in cross wind situations, making it, the ideal empennage to perform the proposed mission.

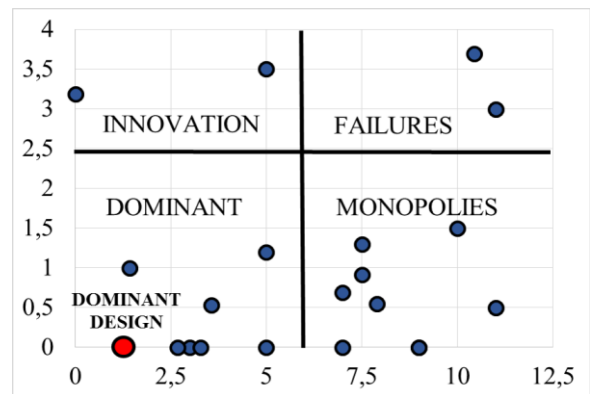
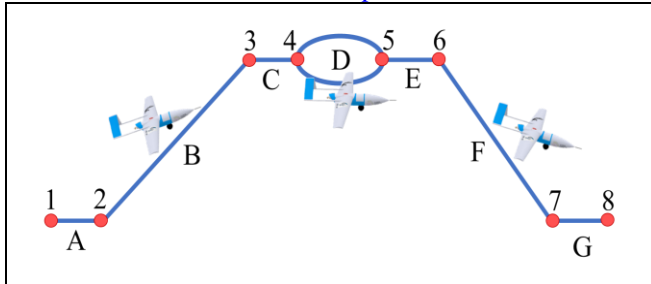


Fig 2. Statistical Entropy Results.

#### 3.2 Mission profile and Weight estimations

After meeting the requirements and restrictions of the **URCUNINA** and taking into account the Galeras Volcano features [8,9]. The proposed mission profile is described according to the Table 1.

**Table 1. Mission Profile Description URCUNINA-UAV.**



Transition points	Flight stage
1. Engine ignition	A. Take-off run
2. Take-off	B. Climb
3. Operational altitude	C. Cruise 1
4. Start Monitoring	D. Volcano monitoring
5. End monitoring	E. Cruise 2
6. Start descent	F. Runway approach
7. Landing	G. Landing
8. Stop the engine	

The ground near the craters is rough and difficult to access [5,10,19]. Therefore, it was assumed an altitude of 2500m to take off at 7 Km from the volcano crater, The **URCUNINA** moves a distance of 2 Km during the climb. Then, it starts the first cruise, moving 12 Km to reach near the crater. The **URCUNINA** should fly around the volcano keeping its altitude, with the aim to monitor the geographical territory over the volcano. Later, it makes a second cruise, returning to the point in which it starts the first cruise and finally its respective descent for landing. In total it spends 120 minutes of operation and covers a distance of 25 Km.

This mission profile was the initial parameter to study the weight estimation of the **URCUNINA**. Therefore, the calculations were performed using a relation between the methodologies proposed by Raymer [22] and Leland [23]. The **URCUNINA** is constituted of several components, which can be divided into sections, such as empty weight ( $W_e$ ), fuel weight ( $W_f$ ) and payload weight ( $W_p$ ). Thus, the equation for the first estimation of the Maximum Take-off Weight ( $MTOW$ ) is:

$$MTOW = W_e + W_f + W_p \quad (1)$$

For the present design, it is of great importance to obtain accurate weight estimations of the components and their distribution. Therefore, the payload weight includes all the main devices

to perform the mission profile, which include an Auto-pilot, several gas sensors, including a miniature mass spectrometer, GPS sensors, photo-video cameras with infrared system and a Data Link, DL, as communication system to control the information obtained, weighing 3.6 Kg. The fuel weight was calculated using the fuel-fraction estimation, according to each phase of flight, then was found the relation ( $W_f/W_o$ ) assuming 6% for reserved and trapped fuel. The ( $W_e$ ) of the **URCUNINA** includes structure and propulsion, finally the empty weight fraction ( $W_e/W_o$ ) can be estimated statistically from the summary of empty-weight by the trend line equations for **UAVs**, with propeller and endurance less than 5 hrs [22,23]. As a result, The  $MTOW = 15.5$  Kg,  $W_e = 7.7$  Kg and  $W_f = 4.2$  Kg.

### 3.3 Constraint Analysis

The constraint analysis involves all the aircraft as a set. It is important to perform this procedure emphasizing on the **UAV** before referring to the wing, because certain parameters in this stage gave the starting point of the wing design. With the values of the weight fractions, it was possible to start the constraint design of the **URCUNINA**, in function of the profile mission.

The main equation [24] for the constraint analysis was simplified for each flight stage: Take-off, Climb, Cruise and Landing. In the Fig. 3 is showed the ( $T/W$ ) ratio and the wing loading ( $W/S$ ) for each flight stage.

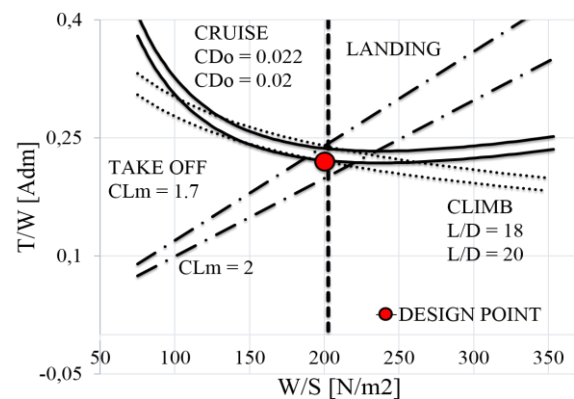


**Fig 3. Constraint Analysis.**

The design point shown in the Fig. 3 was selected in order to minimize the specific power

and the wing loading for each flight phase, with a certain safety margin. The coordinates of the design point are:  $T/W = 0.22$  and  $W/S = 203$  Pa. These parameters was chosen for the beginning of the preliminary aerodynamic design.

#### 4 Preliminary Aerodynamic Design

The constraint analysis indicate that the **URCUNINA** should not exceed  $13.5$  m/s and the takeoff runway have to be less than  $70$ m. These two restrictions presented an iterative design procedure that resulted in a wing surface  $S = 0.75$  m<sup>2</sup> and  $C_L = 1.8$  for stall velocity of  $12.4$  m/s. The *XFLR5* free code was used, for the two-dimensional computational analysis, resolving the velocity field and the pressure distribution around the airfoils by the analysis of flow potential, applying the panels method. A high-lift low Reynolds number airfoil was selected in order to accomplish the constraints registered above. As a consequence, the Eppler 423 high-lift airfoil was chosen. It presented satisfactory results for the present aerodynamic case. For a  $Re = 303000$  at the operating altitude, the  $(C_L)_{max} = 2.2$  at angle of attack  $(AoA) = 20^\circ$ .

The design of the wing platform was conducted with the implementation of the Prandtl's Lifting line theory [11,12,13] aiming to obtain the optimum geometric features that would result in an elliptical wing [25]. According to Phillips [12,13] the lift distribution on a span location of the wings depends directly of the Wingspan ( $b$ ), the Oswald efficiency ( $e$ ), the Aspect Ratio ( $AR$ ) and the Taper ratio ( $\lambda$ ). For this reason, it took into account that an elliptical wing is difficult and expensive to build. Therefore, a taper wing was designed for the **URCUNINA**, trying to keep the induced drag generated by an elliptical wing. To this end, it was found that a  $\lambda = 0.5$ ,  $AR = 11$  and a twist angle of  $-1^\circ$  produced a lift distribution very close to the elliptical fashion. The angle of incidence of the wing was set in  $0.5^\circ$ , where the aerodynamic efficiency of the airfoil is maximized. With these calculations, it was also possible to determine the optimum operational velocity  $V_o = 24$ m/s, which was used in the *CFD* simulations. The wing lift distribution at the operating altitude and the

geometric and aerodynamic characteristics of the wing are summarized in the Fig. 4 and the Table 2 respectively.

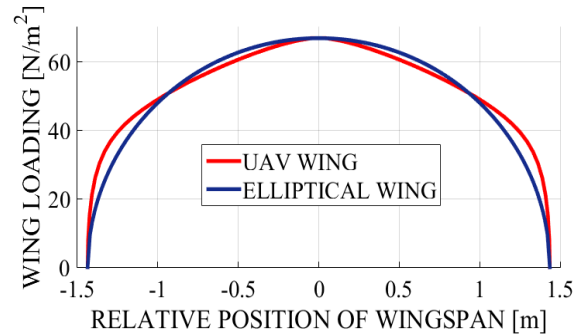


Fig 4. Lift Distribution.

Table 2. Wing Features.

Wingspan [m]	2.872
Root chord length $C_r$ [m]	0.348
Tip chord length $C_t$ [m]	0.174
Mean aerodynamic chord [m]	0.27
Wing Area $S$ [m <sup>2</sup> ]	0.75
Angle of sweep $\Lambda_{c/4}$	0
Airfoil thickness ( $t/c$ )	0.125
Aspect Ratio $AR$	11
Operational Lift Coefficient	0.906
Aerodynamic Efficiency	23.33

#### 4.1 Fuselage Design

The fuselage layout was carried out according to the procedure proposed by Austin [7] in order to have the first estimation of the length  $l_f = 1.16$  m and volume  $V_f = 0.03$ m<sup>3</sup> of the fuselage, according to the *MTOW*. This was designed as a structural support for all the aerodynamic surfaces (Wing, Empennage, Landing Gear and Booms) and also to allow a practical storage of the payload, the fuel tank and a parachute for a vertical landing device.

#### 4.2 Empennage Design

For the empennage design, it was worked with the projected area of the horizontal and vertical stabilizer of a conventional tail without dihedral angle. Therefore, the first estimation of the horizontal stabilizer surface, was  $S_H = 0.074$  m<sup>2</sup> and for the vertical stabilizer surface was  $S_V = 0.0302$  m<sup>2</sup>. The projected area of these dimensions were estimated in *SOLIDWORKS* in

order to obtain a V inverted tail configuration. The airfoil chosen was a *NACA 0012* being ideal in this type of empennage, producing slightly lower drag and sufficient down force to ensure longitudinal stability at low attack angles. In the Fig. 5 is showed the principal dimensions of the **URCUNINA** design. Further information is reported in [26].

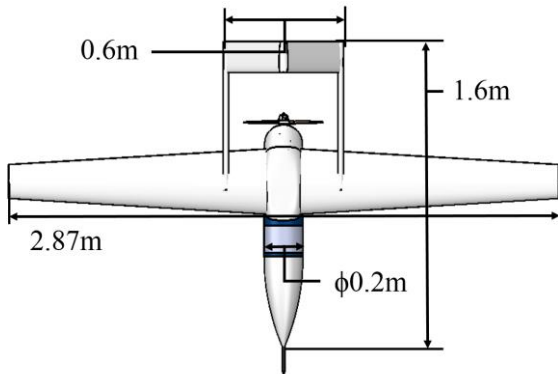


Fig 5. URCUNINA-UAV Dimensions.

### 4.3 Propulsion System

Choosing the most suitable propeller depended of the characteristics of the UAV project. Therefore, three different propellers with fixed pitch were analyzed, with the aim of meeting the performance requirements, having a  $T/W = 0.22$  and  $MTOW = 152.25 N$ . With this type of propellers, not all the engine power is harnessed [27], because of the propeller efficiency. Therefore, the propeller selected provides the maximum values of torque and rotation. After analysis, the 16x8" MASTER propeller was chosen due to its values of Thrust ( $T = 38.76 N$ ) and Efficiency ( $\eta_p = 73\%$ ) in function of the feed ratio. The engine chosen was the 3W 28iCS equipped with an ash filter, aiming to minimize the effect of ash melting in the engine. It is an engine relatively light, weighing 1.2 kg, with a rotational field between 1500 and 8500 rpm.

### 4.4 Drag polar calculation

In this analysis, only the fuselage, the wings, the twin boom and the empennage were considered, in order to make an aerodynamic study only for the main surfaces of the **URCUNINA**. The parasite drag was calculated taking into account the form factor, the wet area and the skin-

friction coefficient of each surface. In this regard, it was analyzed the induced drag component produced by the wing and the empennage was possible to get the drag polar, given by the equation 2.

$$C_D = C_{D0} + kC_L^2 \quad (2)$$

Where:  $C_{D0} = 0.02$

$$k = 1 / (\pi A R e_o) = 0.0395$$

### 4.5 Performance Evaluation

In order to ensure that the propulsion system selected meets with the mission requirements, it was evaluated the available thrust by the engine and the required thrust by the UAV at different altitudes, aiming to know the performance behavior at the operating altitude and its maximum ceiling of operation. In this connection, it was consider that the reduction of the air density generate a lower thrust than the produced at the MSL. In the Fig. 6 is showed the variation of the available and required power at different altitudes in function of the velocity. This results showed that the maximum ceiling of the **URCUNINA** is at 5000m above the sea level. Therefore, it is capable of flying at the operating altitude calculated (4500m), where the minimum velocity at this condition is 12 m/s and the maximum is 26 m/s.

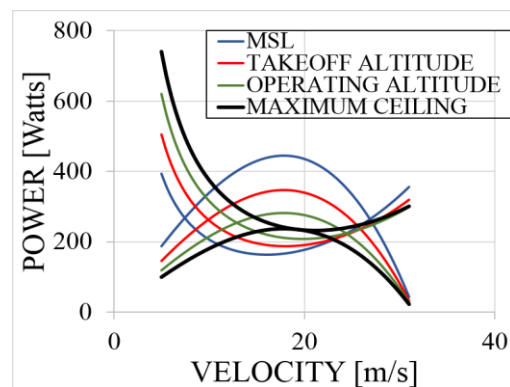


Fig 6. Available and Required Power.

### 4.6 Longitudinal Stability

In this section was ensured that the **URCUNINA** is longitudinally stable. Therefore, the stability contribution of the wing, the empennage and the full configuration were calculated, aiming the condition  $(\partial C_m / \partial \alpha) < 0$ .

As well as the static margin ( $ST$ ) =  $(15.3) \%MAC$  and the neutral point ( $NP$ ) =  $(45.3) \%MAC$  were calculated. As a result, the trim angle ( $\alpha_t$ ) was set in  $4^\circ$ . In the Fig. 7 is showed the moments contribution around CG of the **URCUNINA**.

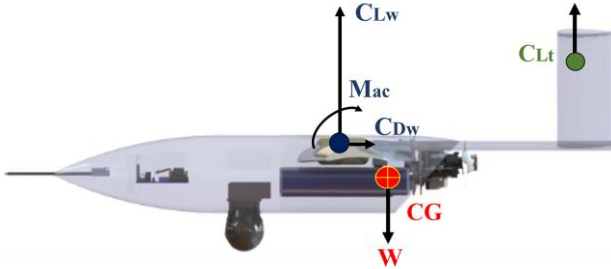


Fig 7. Moments contribution around CG.

## 5 Computational Fluid Dynamics Analysis

This section aims to validate the analytical results obtained in the preliminary aerodynamic design presented above. In this regard, a computational domain was created with  $50m \times 130m \times 20m$  dimensions, in order to obtain a low blocking factor and avoid the restriction of fluid in the simulations.

These were performed with the International Standard Atmosphere (*ISA*) parameters at the operating altitude, using the Shear Stress Transport (*SST*) turbulence model [25,28]. The angle of attack was from  $-4^\circ$  to  $24^\circ$ .

### 5.1 Numerical Approach

Appropriate mesh were calculated for the wing and the full configuration of the **URCUNINA**, discretizing the computational domain in space and time through an adequate number of elements, where the Navier-Stokes equations were solved. Therefore, a grid independence study was conducted. The first layer of cells was set in  $y = 1e^{-4}$  resulting in a  $y^+ \approx 1$ . As a result, approximately  $2.3e^6$  elements for the wing and  $8.0e^6$  elements for the full configuration were generated, using an unstructured mesh (tetrahedral). The Fig. 8 and Fig. 9 show the mesh comparison at different sizes of grid and the final mesh generated for the full configuration, respectively.

The *ANSYS CFX-Solver* [28] was selected to solve the convergence criteria imposed, with the aim to reach the maximum residue adjusted in

$1e^{-5}$ . The maximum number of iterations was 500.

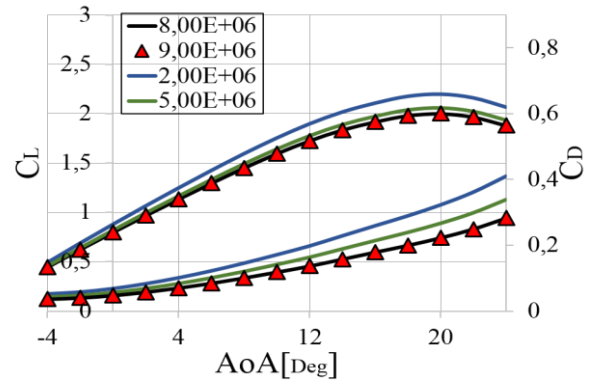


Fig 8. Analysis of independence mesh.

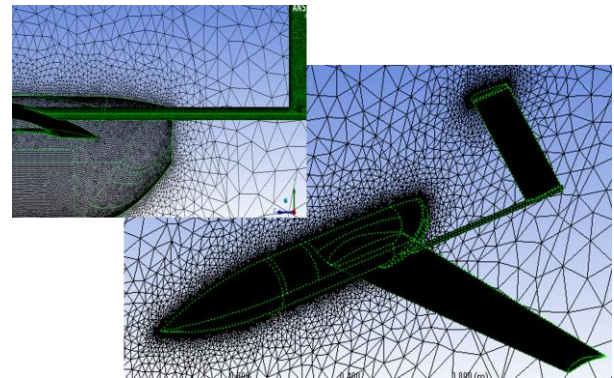


Fig 9. Grid for the **URCUNINA-UAV**.

## 6 Results

In this section the analytical and numerical results of the wing and the full configuration are presented. The simulations were executed in *ANSYS CFX*®.

### 6.1 Lift Coefficient

As can be seen in the Fig. 10, the full configuration presented increase of  $C_L$  than only the wing. This is due to the lift contribution by the empennage configuration (*V inverted tail*) and the fuselage, at attack angles greater than  $10^\circ$ . In the Fig. 11 is showed the streamlines coupled with the pressure contour on the **URCUNINA** at  $0^\circ$ ,  $10^\circ$  and  $20^\circ$  (*Stall angle*), respectively. In the Fig. 11(c) is observed fluid separation on the wing/fuselage junction, this means that the detachment of fluid occurs in distant places of the ailerons, avoiding stall effects in the wingtips. On the other hand, the analytical method (*Lifting Line*) presented similar characteristics, compared with the

numerical results, presenting practically the same lift curve slope ( $dC_L/da$ ) = 4.75rad. However, the  $C_L$  at  $0^\circ$  attack angle was 0.94, unlike both numerical results 0.796 for the full configuration and 0.789 for the wing.

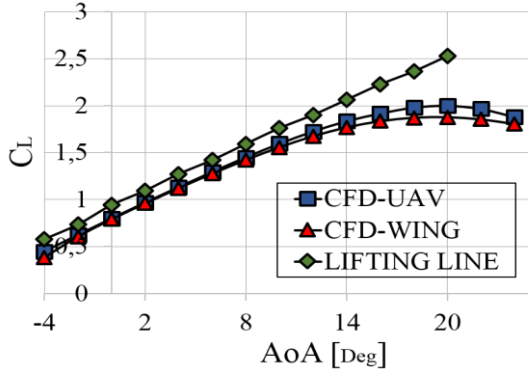


Fig 10.  $C_L$  x AoA.

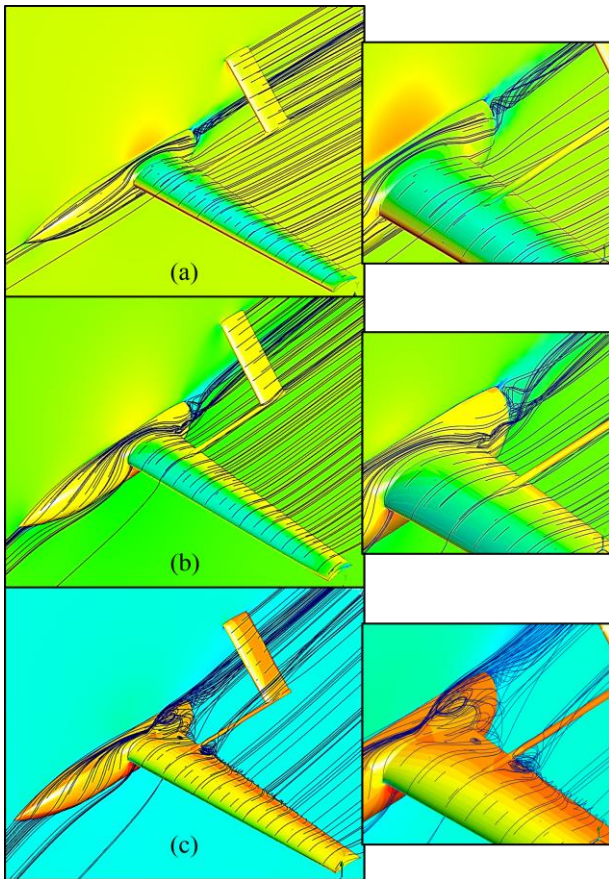


Fig 11. Streamlines at  $0^\circ$  (a),  $10^\circ$  (b) and  $20^\circ$  (c)

## 6.2 Drag Coefficient

As it was expected, the full configuration presented more  $C_D$  than the wing, because of the parasite and interference drag generated by the wing/fuselage junction. The Fig. 12 shows the variation of the  $C_D$  versus angle of attack. The

$C_D$  estimated with the analytical method was calculated with the results of the induced drag and taking into account the drag generated by the 2D simulations of the airfoil as parasite drag. The  $C_D$  at  $0^\circ$  attack angle was 0.037 for the analytic method, 0.035 for the wing simulation and 0.047 for the full configuration.

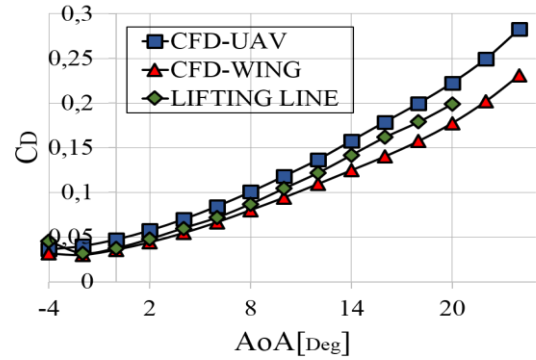


Fig 12.  $C_D$  x AoA.

## 6.3 Moment Coefficient

Despite the increase of lift at attack angles greater than  $10^\circ$ , by the full configuration with respect to the wing, the moment coefficient around the CG of the **URCUNINA** is not affected. In the Fig. 13 is showed that the analytical results evaluated in the longitudinal stability analysis were consistent with the numerical results. In case of the wing,  $(\partial C_m/\partial \alpha)_w > 0$ . Therefore, the longitudinal contribution of the wing is unstable. On the other hand, in the full configuration,  $(\partial C_m/\partial \alpha)_s < 0 \Rightarrow C_{m_{os}} > 0$ . Thus, the **URCUNINA** is statically stable at the flight conditions imposed, respecting its  $(\alpha_i) = 4^\circ$ .

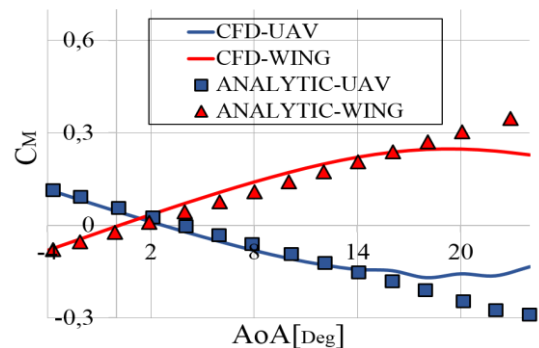


Fig 13.  $C_M$  x AoA.

## 6.4 Aerodynamic Efficiency

The lift to drag ratio curve are presented in the Fig. 14. It is shown that the full configuration



has a maximum efficiency at  $0.5^\circ$  ( $L/D = 17.7$ ). Therefore, the angle of incidence of the wing was imposed correctly on the fuselage of the **URCUNINA**, resulting in an optimal value to be considered in the reducing fuel consumption. Regarding to the wing simulation, the maximum efficiency was set at the same angle of attack. However, the value of  $L/D = 22$ .

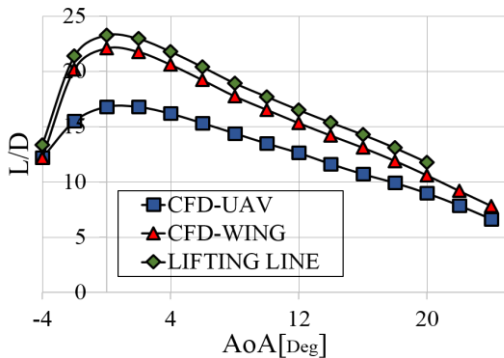


Fig 14. Aerodynamic Efficiency.

### 6.5 Drag Polar

The Drag polar curves can be seen in the Fig. 15. It can be observed that the values obtained in the analytic Lifting Line method were close to the numerical results of the wing. On the other hand, the analytical Drag polar calculated for the main surfaces (wing, fuselage, empennage and booms) of the **URCUNINA** presented similar values, compared with the numerical results of the full configuration. As a consequence, it has an  $L/D = 17.4$  analytical and an  $L/D = 17.7$  numerical for the **URCUNINA**. For the sake of argument, it can be concluded that both the analytical and numerical analysis for the wing platform and the full configuration were performed successfully.

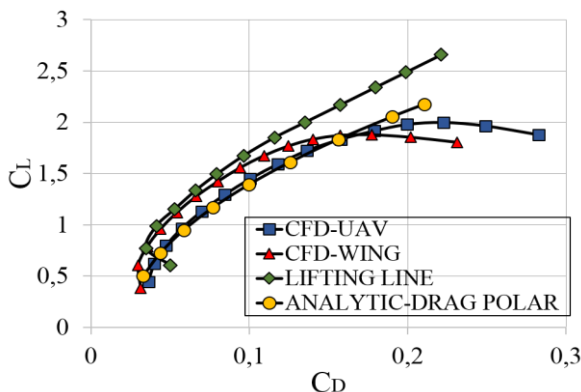


Fig 15. Drag Polar.

### 7 Conclusions

The conceptual and preliminary aerodynamic design of a UAV for superficial volcano monitoring has been carried out. The results obtained with analytical methods have been validated in computational simulations, which show as would be the aerodynamic behavior in mission by the **URCUNINA**. Thus, it was possible to analyze and validate the main findings of the design process, which are summarized in the next statements.

The constraints analysis throughout this work was respected. Therefore, the **URCUNINA** is within the requirements that it can fulfill.

The performance characteristics of the **URCUNINA** show that its maximum ceiling is at  $5000m$ . As a consequence, it could be used in different volcanoes around the world.

Regarding to the aerodynamic coefficients, the numerical results obtained in the simulations are close in relation to the analytical results, verifying that the Eppler 423 airfoil and the V inverted empennage are ideal to perform this kind of mission.

The UAVs are a promising alternative to consider when perform monitoring of volcanoes because in case of an eruption, the use of the **URCUNINA** is to alert the people most at risk near volcanoes and could also be used to give notice to the air traffic control centers about the displacement of the ash/gas plumes, which could affect the commercial and military air operations in the vicinity of the volcanoes, due to the direct impact of volcanic ash on jet aircraft. Furthermore, the **URCUNINA** could serve to reduce the possible damage in the aircraft manned components and avoid the exposition of people to these flight conditions.

By last, experimental analysis are being developed to compare with the analytical and numerical results obtained.

### References

- [1] McNutt S. *Seismic monitoring and eruption forecasting of volcanoes: a review of the state-of-the-art and case histories. Monitoring and mitigation of volcano hazards*, pp 99-146, Springer Berlin Heidelberg, 1996.

- [2] Guffanti M, Casadevall T. Encounters of aircraft with volcanic ash clouds; a compilation of known incidents, 1953-2009. *US Geological Survey*, 2010.
- [3] Diaz J, Pieri D, et al. Unmanned aerial mass spectrometer systems for in-situ volcanic plume analysis. *Journal of the American Society for Mass Spectrometry*, Vol. 26, No. 2, pp 292-304, 2015.
- [4] Patterson M, Mulligan A, et al. Volcano surveillance by ACR silver fox. *American Institute of Aeronautics and Astronautics Infotech@ Aerospace Conference*, Arlington, Virginia, USA, pp 26-29, 2005.
- [5] Pieri D, et al. In situ observations and sampling of volcanic emissions with NASA and UCR unmanned aircraft, including a case study at Turrialba Volcano, Costa Rica. *Geological Society, London, Special Publications*, Vol. 380, No. 1, pp 321-352, 2013.
- [6] Bravo P, et al. Parametric conceptual design of a UAV for superficial volcano monitoring. *23<sup>rd</sup> ABCM International Congress of Mechanical Engineering*, Rio de Janeiro, Brazil, Vol. 23, paper number 679, 2015.
- [7] Austin R. *Unmanned aircraft systems: UAVS design, development and deployment*. 1<sup>st</sup> edition, John Wiley & Sons, 2011.
- [8] Cortés G, Raigosa J. A synthesis of the recent activity of Galeras volcano, Colombia: Seven years of continuous surveillance, 1989–1995. *Journal of volcanology and geothermal research*, Vol. 77, No. 1, pp 101-114, 1997.
- [9] Ordón M, et al. Morphological changes of the active cone of Galeras volcano, Colombia, during the last century. *Journal of volcanology and geothermal research*, Vol. 77, No. 1, pp 71-87, 1997.
- [10] Diaz J, Corrales E, et al. Volcano monitoring with small unmanned aerial systems. *American Institute of Aeronautics and Astronautics Infotech@ Aerospace Conference*, Garden Grove, California, USA, paper number 2522, 2012.
- [11] Glauert H. *The elements of aerofoil and airscrew theory*. Cambridge University Press, 1983.
- [12] Phillips W. Lifting-line analysis for twisted wings and washout-optimized wings. *Journal of aircraft*, Vol. 41, No. 1, pp 128-136, 2004.
- [13] Phillips W, et al. Minimizing Induced Drag with Geometric and Aerodynamic Twist, CFD Validation. *43rd AIAA Aerospace Sciences Meeting and Exhibit*, Reno, Nevada, USA, paper number 1034, 2005.
- [14] Selig M, Guglielmo J. High-lift low Reynolds number airfoil design. *Journal of aircraft*, Vol. 34, No. 1, pp 72-79, 1997.
- [15] Liebeck R. Design of subsonic airfoils for high lift. *Journal of aircraft*, 1978, vol. 15, no 9, p. 547-561.
- [16] Smith A. High-lift aerodynamics. *Journal of Aircraft*, Vol. 12, No. 6, pp 501-530, 1975.
- [17] Diaz J, Giese D, et al. Mass spectrometry for in-situ volcanic gas monitoring. *Trends in Analytical Chemistry*, Vol. 21, No. 8, pp 498-514, 2002.
- [18] Johnson B, et al. In situ observations of volcanic ash clouds from the FAAM aircraft during the eruption of Eyjafjallajökull in 2010. *Journal of Geophysical Research: Atmospheres*, Vol. 117, No. D20, 2012.
- [19] Caltabiano D, et al. Architecture of a UAV for volcanic gas sampling. *Emerging Technologies and Factory Automation - 10th IEEE Conference*, Catania, Italy, Vol. 1, paper number 744, 2005.
- [20] Weber K, et al. Airborne in-situ investigations of the Eyjafjallajökull volcanic ash plume on Iceland and over north-western Germany with light aircrafts and optical particle counters. *Atmospheric Environment*, Vol. 48, pp 9-21, 2012.
- [21] Abdalla A. *Multidisciplinary optimization for conceptual design of aircraft based on evolutionary heuristics and decision making*. PhD thesis, Engineering School of São Carlos, University of São Paulo, 2009.
- [22] Raymer D. *Aircraft design: a conceptual approach*. American Institute of Aeronautics and Astronautics Inc, 1992.
- [23] Leland N. *Fundamentals of Aircraft and Airship Design*. American Institute of Aeronautics and Astronautics, 2010.
- [24] Mattingly Jack. *Aircraft Engine Design*. American Institute of Aeronautics and Astronautics, Inc. Reston, 2002.
- [25] Kontogiannis S. Design, performance evaluation and optimization of a UAV. *Aerospace Science and Technology*, Vol. 29, No. 1, pp 339-350, 2013.
- [26] Bravo P, Uribe A. *Conceptual and preliminary design of a UAV for superficial volcano monitoring*. Aeronautical engineering dissertation, Engineering School of São Carlos, University of São Paulo, 2015.
- [27] Anderson J. *Aircraft performance and design*. Boston: WCB/McGraw-Hill, 1999.
- [28] ANSYS Inc. *ANSYS CFX-Solver Modeling Guide*. November, 2010.

## 8 Contact Author Email Address

mailto: pdbravom@usp.br  
 mailto: pfalvaro@sc.usp.br

## Copyright Statement

The authors confirm that they, and/or their company or organization, hold copyright on all of the original material included in this paper. The authors also confirm that they have obtained permission, from the copyright holder of any third party material included in this paper, to publish it as part of their paper. The authors confirm that they give permission, or have obtained permission from the copyright holder of this paper, for the publication and distribution of this paper as part of the ICAS 2016 proceedings or as individual off-prints from the proceedings.